

## On the Feedback of the Rhines–Young Pool on the Ventilated Thermocline\*

ZHENGYU LIU AND JOSEPH PEDLOSKY

*Department of Physical Oceanography, Woods Hole Oceanographic Institution, Woods Hole, Massachusetts*

DAVID MARSHALL\*\*

*Department of Earth, Atmospheric and Planetary Sciences, Massachusetts Institute of Technology, Cambridge, Massachusetts*

TORNSTER WARNCKE

*Alfred Wegener Institute, Bremerhaven, Germany*

19 August 1991 and 9 July 1992

### ABSTRACT

The model developed by Pedlosky and Young is used to investigate the feedback of a Rhines–Young pool on a ventilated thermocline. It is found that the potential vorticity gradient in a ventilated layer is reduced due to the nonlinear coupling with a deep Rhines–Young pool. Physically, this occurs because part of the Sverdrup transport is carried by the deep pool. As a result, the subduction velocity, and in turn, the potential vorticity gradient of the subducted water, is decreased.

The coupling between the classical Rhines–Young pool (Rhines and Young 1982) and the ventilated thermocline (Luyten et al. 1983) has remained an interesting topic in general oceanic circulation. In an effort to marry the two theories, Pedlosky and Young (1983) (hereafter referred as PY) found that adding a ventilated thermocline atop a Rhines–Young pool tends to reduce the size of the deep pool zone. In this note, we will explore the other aspect of the issue, namely, the effect of a deep pool on the ventilated thermocline above.

Following PY, we adopt a 3.5-layer model. A schematic view of the geometry of the model is shown in Fig. 1. More details of the model can be found in PY. The notation is changed slightly. From the top to the bottom, we will refer to the three layers as layer one, layer two, and layer three, respectively. All quantities in each layer are subscripted with the layer number. The northern boundary of the subtropical gyre is denoted by  $f_n$ , while the outcrop line of the top layer is denoted by  $f_1$ . For simplicity, we further assume the

same reduced gravity in each layer, that is,  $\gamma_n \equiv (\rho_n - \rho_{n-1})g/\rho_0 = \gamma$ ,  $n = 1, 2, 3$ , where  $\rho_0$  is the standard density. The dynamic pressures in each layer are

$$\begin{aligned} \frac{p_3}{\rho_0} &= \gamma(h_1 + h_2 + h_3), & \frac{p_2}{\rho_0} &= \frac{p_3}{\rho_0} + \gamma(h_1 + h_2), \\ \frac{p_1}{\rho_0} &= \frac{p_2}{\rho_0} + \gamma h_1. \end{aligned} \quad (1)$$

The solution can be derived in different regions as suggested by PY. North of the outcrop line,  $f \geq f_1$ , only layer two and layer three exist (or  $h_1 = 0$ ). There are two regions (see Fig. 2). Adjacent to the eastern boundary is the shadow zone of layer three (denoted  $S^3$ ), in which layer three is motionless and the layer thickness of layer-two  $h_2$  and layer-three  $h_3$  can be derived as

$$h_2 = \sqrt{D^2 + H_2^2}, \quad (2a)$$

$$h_2 + h_3 = H_2 + H_3 \quad (2b)$$

where

$$D^2 = 2f^2 w_e(f)x/\beta\gamma. \quad (3)$$

Here, the eastern boundary is set at  $x = 0$ . To the west of  $S^3$  is the Rhines–Young pool (denoted as  $P^3$ ) with a uniform potential vorticity in layer three, whose solution is

$$h_3 = \frac{f}{f_n} H_3, \quad (4a)$$

\* Woods Hole Oceanographic Institution Contribution Number 7816.

\*\* On leave from: Space and Atmospheric Physics Group, Imperial College, London.

Corresponding author address: Dr. Zhengyu Liu, Princeton University, Sayer Hall, P.O. Box CN 710, Princeton, NJ 08544-0710.

$$h_2 = \frac{1}{2} \{ -h_3 + \sqrt{2[D^2 + (H_2 + H_3)^2 + H_2^2] - h_3^2} \}. \tag{4b}$$

These two regions are separated by the pool zone boundary  $x_P(f)$  determined from  $D^2[x_P(f), f] = 2H_2H_3(1 - f/f_n) + (1 - f/f_n)^2H_3^2$ .

South of the outcrop line, the solution is more complicated. The general approach has been outlined in PY. We will highlight the principle here and leave the detailed solutions to the Appendix. As shown in Fig. 2, there is a shadow zone of layer three ( $S^2$ ) near the eastern boundary, which is bounded by the shadow zone boundary  $x_S$ . West of  $S^2$  is the ventilated zone of layer two; however, because of different circulations in layer three and different subduction water sources, there will be three subzones (Fig. 2). Next to  $S^2$  is the classical LPS ventilated zone ( $V_{S^3}^2$ ) in which layer three is at rest (i.e., in  $S^3$ ) up to the outcrop line. Above the deep pool ( $P^3$ ), all three layers are in motion and layer-two water subducts from the part of the outcrop line west of the pool zone boundary. The structure is different from the classical ventilated zone and will be denoted by ( $V_{P^3}^2$ ). Finally, there is a buffer zone between  $V_{P^3}^2$  and  $V_{S^3}^2$ , in which the water of the second layer subducts from the same source as that of  $V_{P^3}^2$ , but now layer three is at rest like  $V_{S^3}^2$ . This buffer zone will be denoted as  $V_{S^3}^{2B}$ . The buffer zone  $V_{S^3}^{2B}$  is separated from the LPS ventilated zone  $V_{S^3}^2$  by  $x_B$ . When the outcrop line moves northward, the size of the buffer zone increases at the expense of the LPS ventilated zone. This implies a strong coupling between the deep pool zone and the ventilated zone. In the limiting case  $f_1 \rightarrow f_n$ , the LPS ventilated zone vanishes and the ventilated zone consists of  $V_{S^3}^2$  and  $V_{P^3}^2$  only. On the other hand, if the outcrop line is south enough such that the layer-three pool zone will not extend to the outcrop

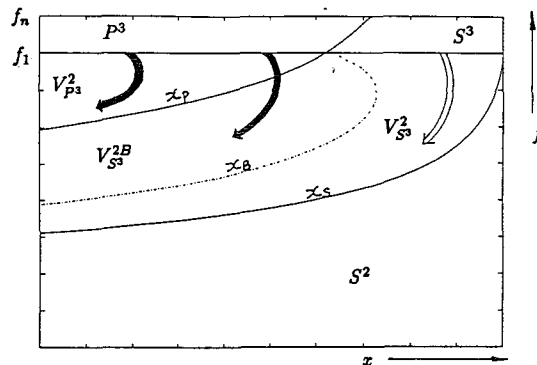


FIG. 2. A schematic figure of different zones in the model. The different flows in layer two are also drawn. See the text for a fuller discussion. The solid arrows represent flow subducting above the pool zone; the blank arrow represents the flow subducting above the shadow zone.

line, there will be no buffer zone. Therefore, the deep pool zone is decoupled from the ventilated zone. It should be pointed out that, physically, the buffer zone is the same as the LPS ventilated zone because both have layer-two waters flowing above a motionless shadow zone  $S^3$ . Thus, in layer two, we have three physical regions: the motionless shadow zone ( $S^2$ ), the ventilated zone ( $V_{P^3}^2$ ) above a pool zone, and a ventilated zone ( $V_{S^3}^2$  and  $V_{S^3}^{2B}$ ) above a motionless shadow zone. Finally, if the outcrop line is north of the maximum Ekman pumping, a region appears with the second-layer potential vorticity contours closed to the western boundary. Luyten et al. (1983) assumed that the potential vorticity is uniform and also called this region a pool zone (in our model, this pool zone has a uniform potential vorticity in the second layer and should be denoted as  $P^2$  in distinguishing from the deep pool in layer-three  $P^3$ ). This region is not discussed in this note since it will not affect our conclusion.<sup>1</sup>

An important effect of the deep pool on the ventilated thermocline is seen if the second layer potential vorticity  $q_2$  (Fig. 3a) is compared with that of an LPS ventilated thermocline (Fig. 3b). East of  $x_B$ , both solutions are exactly the same. West of  $x_B$ , however, the potential vorticity field in Fig. 3a is more uniform than that in Fig. 3b. Indeed, the  $q_2$  gradient west of  $x_B$  is reduced by a factor of about 2 to 3 compared with that

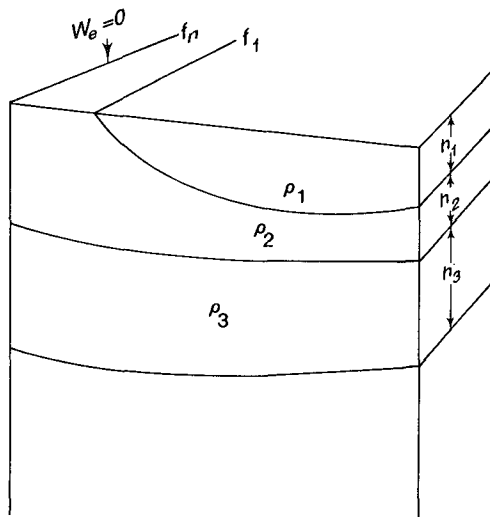


FIG. 1. A schematic view of the geometry of the 3.5-layer model. See the text for notations.

<sup>1</sup> In a layered model, if the outcrop line  $f_1$  approaches the gyre boundary  $f_n$ , the layer-two pool zone expands while the layer-two ventilated zone vanishes (Talley 1985). This is not the case of our interest in this note because of the vanishing ventilated zone. Now, instead of being dominated by the coupling between a ventilated layer and a deep pool, the coupling between layer two and layer three becomes essentially the coupling between the two pool zones in layer two and layer three. Furthermore, if the model is modified by adding a mixed layer with a finite thickness on the top, the size of the layer-two pool zone will always be reduced (Pedlosky and Robbins 1991). Therefore, the coupling between a ventilated zone and a deep pool zone will be stronger than the present layered model, which does not have a mixed layer.

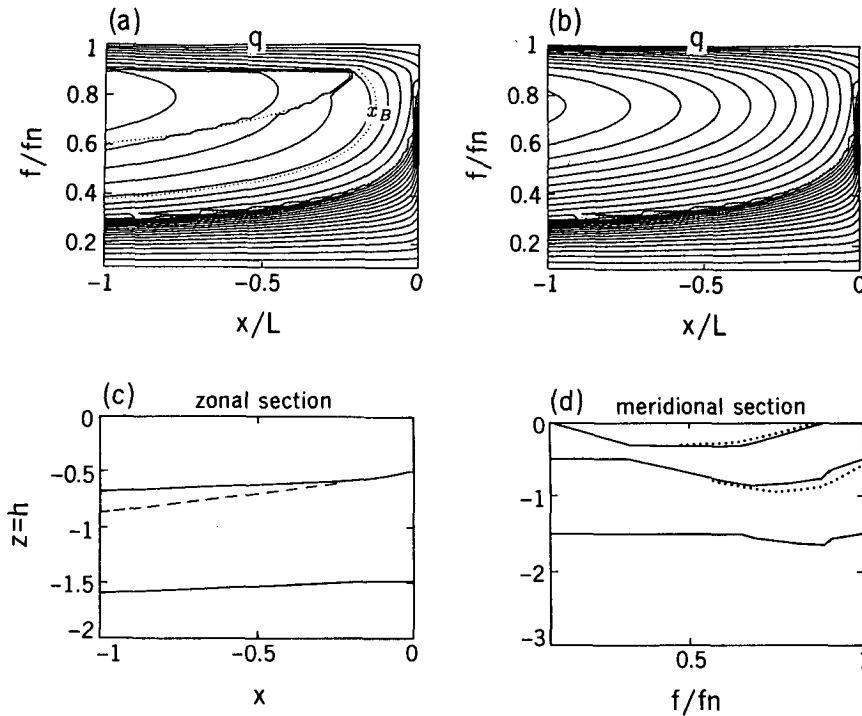


FIG. 3. Layer-two potential vorticity, zonal, and meridional sections of the cases with the outcrop line at  $f_1 = 0.9f_n$  (the outcrop line is not drawn). The Ekman pumping takes the form  $w_e(f) = -\sin[\pi(f - f_s)/(f_n - f_s)]$ ;  $f_s = 0.1f_n$  is the southern boundary of the subtropical gyre. (a) Layer-two potential vorticity in the presence of a deep pool zone.  $H_2 = 0.5H$ ,  $H_3 = H$  are chosen, where  $H = 2f_n^2 L / \beta\gamma$ . Here  $L$  is the dimensional scale in  $x$ . The western boundary is set at  $x = -L$ . The dotted lines show, from east to west, the shadow zone boundary  $x_s$ , the buffer zone boundary  $x_B$ , and the pool zone boundary  $x_P$ , respectively;  $x_B$  is labeled. (b) Same as (a) but for a LPS ventilated thermocline (without a deep pool)  $H_2 = 0.5H$ ,  $H_3 \gg H$ . Only  $x_s$  exists. The contour intervals in (a) and (b) are the same. (c) The zonal section along the outcrop line  $f_1$ . Solid lines are for the case in (a) with a pool zone. Dashed line is for the case in (b) without a pool zone. (d) The meridional section at  $x = -0.7L$ . Solid lines are for the case in (a) with a deep pool and dotted lines are for the case in (b) without a deep pool.

in Fig. 3b. Therefore, the effect of the deep pool zone on the ventilated thermocline is to decrease the potential vorticity gradient in the ventilated zone.

The physics is simple. Since the second-layer potential vorticity in the ventilated zone is set on the outcrop line, we can concentrate on the outcrop line. On the section along the outcrop line,  $h_1 = 0$ . In the LPS ventilated thermocline, layer three is at rest (as in  $V_{33}^2$ ). Thus, all the Sverdrup transport has to be carried in layer two by a strong meridional velocity. Geostrophic balance then requires a rapid thickening of  $h_2$  westward or a strong  $q_2 = f_1/h_2$  gradient. In contrast, above the pool zone along the outcrop line, part of the Sverdrup transport is shared by layer three, which circulates in the pool. Consequently, layer two has a weaker meridional velocity and in turn a smaller potential vorticity

gradient. This can be seen in Fig. 3c, where the layer depths along the outcrop line are drawn for both the case with a pool zone (solid lines) and the case without a pool zone (dashed line). In the part east of the pool zone, the layer-two depth is the same as the case in the absence of a deep pool zone. Above the deep pool zone, however, the zonal slope of the layer-two depth becomes smaller than the case without a pool zone. This gives the reduced subduction potential vorticity gradient in Fig. 3a. To provide a clear picture of the solution, a meridional section of the solutions with and without a deep pool is also presented in Fig. 3d.

The reduction of  $q_2$  gradient can be estimated by calculating  $q_2$  along the outcrop line. In the LPS ventilated thermocline, along the outcrop line,  $h_{2LPS}$  is given in (2a). With a pool zone, the  $h_2$  is determined in (4a,b). Thus, we have the ratio

$$R \equiv \frac{\partial h_2 / \partial x}{\partial h_{2LPS} / \partial x} = \frac{\partial h_2 / \partial D^2}{\partial h_{2LPS} / \partial D^2} = \frac{\sqrt{D^2 + H_2^2}}{\left\{ 2(D^2 + H_2^2) + 2H_2^2 + 4H_2H_3 + \left[ 2 - \left( \frac{f}{f_n} \right)^2 \right] H_3^2 \right\}^{1/2}}, \text{ on } f = f_1. \quad (5)$$

It is easily seen that the ratio has an upper bound  $R_{\max}$

$$R \leq R_{\max} = \frac{1}{\sqrt{2}} < 1. \tag{6}$$

Therefore, the potential vorticity gradient is always reduced due to the pool zone by at least a factor of  $\sqrt{2}$ . More generally, if we take  $D^2 \approx H_2^2 \approx H_3^2$ , (6) gives an estimate of the reduction rate

$$R < \frac{1}{\sqrt{6}}, \tag{7}$$

where  $(f_1/f_n)^2 \ll 2$  has been used. Furthermore, near the northern boundary when  $f_1 \rightarrow f_n$ , we have  $D^2 \rightarrow 0$ . Assuming  $H_2 = H_3$ , we have  $R \rightarrow 1/3$ , giving a larger reduction of the subduction potential vorticity. This occurs because when the outcrop line moves toward the northern boundary, the buffer zone becomes larger. In other words, there is a strong coupling between the pool zone and the ventilated zone. Hence, in general, we should expect a reduction by a factor of about 2 to 3.

The finding in this note suggests the following picture on a ventilated isopycnal. Adjacent to the eastern boundary, there is a strong potential vorticity gradient in the shadow zone. To the west of the shadow zone is the LPS ventilated zone, which has a potential vorticity gradient much weaker than that of the shadow zone. Farther west is the ventilated region including both  $V_{p_3}^2$  and  $V_{S^2}^2$ , which are coupled with the deep Rhines-Young pool. In this region waters subduct above the pool along the outcrop line. The potential vorticity gradient is reduced by about a factor of 2 to 3 compared with the LPS ventilated zone. When the outcrop line is moved northward, the size of the buffer zone increases. Thus, one should expect an eastward expansion of the weak potential vorticity gradient region. Finally, in the westernmost region, layer two has a pool zone where the coupling with the deep pool has different dynamics. This is not discussed in this note. The above discussion presents a picture of a westward gradually reduced potential vorticity gradient. Weak potential vorticity gradients are to be expected even on ventilated isopycnals because of the nonlinear coupling with unventilated layers.

It should be pointed out that other mechanisms could also make the potential vorticity in a ventilated zone more uniform. Some numerical experiments of eddy-resolving models suggest that eddy mixing tends to homogenize the potential vorticity on a ventilated isopycnal (Cox 1985; Boning and Cox 1988). Furthermore, we have adopted a zonal outcrop line here. Observations show, however, that outcrop lines in a subtropical gyre tend to tilt in the southeast-northwest direction. This orientation of outcrop line also favors a subduction potential vorticity more uniform than that of a zonal outcrop line (e.g., Williams 1991) and therefore offers another mechanism for a reduced po-

tential vorticity gradient in the ventilated zone. All of these suggest that the weak potential vorticity gradients observed on isopycnals of subtropical gyres in both observations and numerical experiments need not necessarily imply the existence of homogenized potential vorticity pool with geostrophic contours closed to the western boundary.

*Acknowledgments.* The authors appreciate the criticisms and suggestions of two anonymous reviewers. This work is partly supported by Division of Atmospheric Sciences, NSF (ZL and JP), and partly supported by Natural Environment Research Council, U.K. (DM). This work results from our activities at the Summer School on Environmental Dynamics 1991 in Venice, Italy. This school was supported by grants from the Italian National Research Council (CNR) and from the Istituto Veneto. The authors thank both institutions for their generous hospitality.

APPENDIX

The Solution in a 3.5-Layer Model

South of the outcrop line ( $f \leq f_1$ ), there are four regions,  $S^2$ ,  $V_{S^2}^2$ ,  $V_{S^2}^{2B}$ ,  $V_{p_3}^2$  (see Fig. 2 and the discussion in the text). The solution in the shadow zone  $S^2$  is simply (see PY)

$$h_1 = \sqrt{D^2}, \tag{A1a}$$

$$h_2 = H_2 - h_1, \tag{A1b}$$

$$h_3 = H_3. \tag{A1c}$$

The shadow zone boundary is determined by

$$D^2[x_S(f), f] = [1 - (f/f_1)]H_2^2.$$

East of the shadow zone is the ventilated zone where potential vorticity of layer two is conserved. Note Eq. (1), we have

$$q_2 = \frac{f}{h_2} = G(p_2) = G(h_1 + h_2 + h_3 + h_1 + h_2). \tag{A2}$$

The function  $G$  is determined on the outcrop line  $f = f_1$  by ( $h_1 = 0$ )

$$\frac{f_1}{h_2} = G(h_2 + h_3 + h_2). \tag{A3}$$

Along the outcrop line, east of the  $x_P(f_1)$ , layer three is at rest. Thus, layer-three pressure and the Sverdrup relation are

$$p_3 = h_1 + h_2 + h_3 = H_2 + H_3, \tag{A4a}$$

$$(h_1 + h_2)^2 + h_1^2 = D^2 + H_2^2. \tag{A4b}$$

Using (A4a), (A3) gives

$$G(\mu) = \frac{f_1}{\mu - (H_2 + H_3)}. \tag{A5}$$

This yields the solution in the classical ventilated zone  $V_{S^3}^2$  as (see PY)

$$h_1 + h_2 = \frac{\sqrt{D^2 + H_2^2}}{\sqrt{1 + [1 - (f/f_1)]^2}}, \quad (A6a)$$

$$h_1 = [1 - (f/f_1)][h_1 + h_2], \quad (A6b)$$

$$h_3 = H_2 + H_3 - (h_1 + h_2). \quad (A6c)$$

Above the pool zone is  $V_{P^3}^2$ . Layer three has a uniform potential vorticity. Thus,

$$h_3 = \frac{f}{f_n} H_3. \quad (A7)$$

Equation (A7) also holds on the outcrop line. Thus, using (A7), (A4) determines the  $G$  function as

$$G(\mu) = 2f_1 \left/ \left( \mu - \frac{f_1}{f_n} H_3 \right) \right. \quad (A8)$$

This  $G$  is different from that in (A5), reflecting the fact that the subducted waters have different properties. Now all the three layers are moving, so the Sverdrup relation is

$$(h_1 + h_2 + h_3)^2 + (h_1 + h_2)^2 + h_1^2 = D^2 + (H_2 + H_3)^2 + H_2^2, \quad (A9)$$

which differs from (A4b). The solution in  $V_{P^3}^2$  is then obtained as

$$h_1 = \left( \frac{f_1}{f} - 1 \right) h_2 + \frac{H_3}{2f_n} (f_1 - f), \quad (A10a)$$

$$h_2 = \frac{1}{2} [-h_3 + \sqrt{h_3^2 - 4d}], \quad (A10b)$$

where  $h_3$  is determined in (A7) and

$$d = \frac{f^2}{f_1^2 \{2 + [1 - (f/f_1)]^2\}} \left\{ \frac{f_1^2}{4f_n^2} H_3^2 [1 + (f/f_1)] \times [3 - 2(f/f_1)] - \{D^2 + H_2^2 + [H_2 + H_3]^2\} \right\}.$$

The pool zone boundary is determined by  $D^2[x_P(f), f] = 2H_2H_3(1 - f/f_n) + (1 - f/f_n)^2H_3^2 + h_1^2(x_P(f), f)$ . Finally, in the buffer zone  $V_{S^3}^2$ , the water comes from the same source as  $V_{P^3}^2$ , so the  $G$  function is the same as in (A8). However, now layer three is at rest. Therefore, like in  $V_{S^3}^2$ , the pressure in layer three and the Sverdrup relation are determined in (A4a,b). Substituting (A4a) and (A8) into (A3), we obtain

$$\frac{f}{h_2} = 2f_1 \left/ \left( H_2 + H_3 + h_1 + h_2 - \frac{f_1}{f_n} H_3 \right) \right. \quad (A11)$$

Substitution of (A10) and (A5a) into (A5b), we have

$$h_1 + h_2 = \frac{1}{2A} (-B + \sqrt{B^2 - 4AC}), \quad (A12)$$

where

$$A = 1 + \left( 1 - \frac{f}{2f_1} \right)^2,$$

$$B = -\frac{f}{f_1} \left( 1 - \frac{f}{2f_1} \right) \left[ H_2 + \left( 1 - \frac{f_1}{f_n} H_3 \right) \right],$$

$$C = \frac{f^2}{4f_1^2} \left[ H_2 + \left( 1 - \frac{f_1}{f_n} H_3 \right) \right]^2 - (D^2 + H_2^2).$$

Equations (A4a), (A11), and (A12) give the solution in the buffer zone. The continuity of layer thickness from the buffer zone to the  $V_{S^3}^2$  yields the buffer zone boundary

$$D^2[x_B(f), f] = -H_2^2 + \frac{1}{2a} (-b + \sqrt{b^2 - 4aE^2}),$$

where

$$a = \left\{ 1 - \frac{A}{1 + [1 - (f/f_1)]^2} \right\}^2,$$

$$b = \frac{2EA - B^2}{1 + [1 - (f/f_1)]^2} - 2E,$$

$$E = \frac{f^2}{4f_1^2} \{ H_2 + [1 - (f_1/f_n)] H_3 \}^2.$$

REFERENCES

Boning, C. W., and M. D. Cox, 1988: Particle dispersion and mixing of conservative properties in an eddy-resolving model. *J. Phys. Oceanogr.*, **18**, 320-338.  
 Cox, M. D., 1985: An eddy resolving numerical model of the ventilated thermocline. *J. Phys. Oceanogr.*, **15**, 1312-1323.  
 Luyten, J. L., J. Pedlosky, and H. Stommel, 1983: The ventilated thermocline. *J. Phys. Oceanogr.*, **13**, 292-309.  
 Pedlosky, J., and W. R. Young, 1983: Ventilation, potential-vorticity homogenization and the structure of the ocean circulation. *J. Phys. Oceanogr.*, **13**, 2020-2036.  
 —, and P. Robbins, 1991: The role of finite mixed-layer thickness in the structure of the ventilated thermocline. *J. Phys. Oceanogr.*, **21**, 1018-1031.  
 Rhines, P. B., and W. R. Young, 1982: A theory of the wind-driven circulation I. Mid-Ocean Gyres. *J. Mar. Res.*, **40**(Suppl), 559-596.  
 Talley, L. D., 1985: Ventilation of the subtropical North Pacific: The shallow salinity minimum. *J. Phys. Oceanogr.*, **15**, 633-649.  
 Williams, R. G., 1991: The role of the mixed layer in setting the potential vorticity of the main thermocline. *J. Phys. Oceanogr.*, **21**, 1003-1013.